Available online at www.sciencedirect.com
ScienceDirect
International Journal of Thermal Sciences 47 (2008) 431–441
International Journal of Thermal Sciences
www.elsevier.com/locate/ijts

Forecasting of a ground-coupled heat pump performance using neural networks with statistical data weighting pre-processing

Hikmet Esen [a,*], Mustafa Inalli [b], Abdulkadir Sengur [c], Mehmet Esen [a]

[a] *Department of Mechanical Education, Faculty of Technical Education, Firat University, 23119 Elazig, Turkey*
[b] *Department of Mechanical Engineering, Faculty of Engineering, Firat University, 23279 Elazig, Turkey*
[c] *Department of Electronic and Computer Science, Faculty of Technical Education, Firat University, 23119 Elazig, Turkey*

Received 2 November 2006; received in revised form 2 March 2007; accepted 2 March 2007

Available online 18 April 2007

Abstract

The objective of this work is to improve the performance of an artificial neural network (ANN) with a statistical weighted pre-processing (SWP) method to learn to predict ground source heat pump (GCHP) systems with the minimum data set. Experimental studies were completed to obtain training and test data. Air temperatures entering/leaving condenser unit, water-antifreeze solution entering/leaving the horizontal ground heat exchangers and ground temperatures (1 and 2 m) were used as input layer, while the output is coefficient of performance (COP) of system. Some statistical methods, such as the root-mean squared (RMS), the coefficient of multiple determinations (R^2) and the coefficient of variation (cov) is used to compare predicted and actual values for model validation. It is found that RMS value is 0.074, R^2 value is 0.9999 and cov value is 2.22 for SCG6 algorithm of only ANN structure. It is also found that RMS value is 0.002, R^2 value is 0.9999 and cov value is 0.076 for SCG6 algorithm of SWP-ANN structure. The simulation results show that the SWP based networks can be used an alternative way in these systems. Therefore, instead of limited experimental data found in literature, faster and simpler solutions are obtained using hybridized structures such as SWP-ANN.

Keywords: Artificial neural network; Ground coupled heat pump performance; Forecast; Data pre-process

1. Introduction

GCHP systems have received considerable attention in recent decades as an alternative energy source for residential and commercial space heating and cooling applications. GCHP utilises the energy storage capacity of the ground to provide highly efficient heating, cooling and hot water for many different types of buildings enabling major reductions in electrical and gas consumption to be achieved. This technology has a lower environmental force than any conventional system, with GCHPs offering the lowest CO_2 emission count for heating products, and a very low liability for Carbon Taxes. A GCHP system uses the world's largest heat reserve, storage facility and solar collector—the earth itself. The ground is able to provide free cooling, a heat source and a heat sink, enabling major environmental benefits to be achieved. Surplus heat generated in the building in summer months is effectively stored in the earth and used to improve the efficiency during the heating season. Heat extracted from the ground and used in the building during winter months gives the free cooling ability and higher efficiency mechanical cooling in high summer. The ground heat exchanger (GHE) used in conjunction with a closed-loop GCHP system consists of a system of long plastic pipes buried vertically or horizontally in the ground [1,2].

Forecasting of performance is important in many heat pump applications. It is recommended that ANN can be used to predict the performances of thermal systems in engineering applications. Accurate heat pump system performance forecasting is the precondition for the optimal control and energy saving operation of Heating, Ventilating and Air-Conditioning (HVAC) systems. Especially for those systems that use thermal storage technology, heat pump performance forecasting

* Corresponding author. Tel.: +90 424 237 0000/4228; fax: +90 424 236 7064.
E-mail address: hikmetesen@firat.edu.tr (H. Esen).

1290-0729/$ – see front matter
doi:10.1016/j.ijthermalsci.2007.03.004

Nomenclature

ANN	Artificial neural network
COP	heating coefficient of performance of ground coupled heat pump system
cov	coefficient of variation ..... %
$C_{p,air}$	specific heat of air ..... kJ/kg K
n	number of independent data patterns
RMS	root-mean square error
R^2	fraction of variance
SCG	scaled conjugate gradient learning algorithm
SWP	statistical weighted pre-processing
t	target neural network output
T_a	outdoor air temperature ..... °C
T_i	indoor air temperature ..... °C
T_{g1}	temperature of ground at 1 m depth ..... °C
T_{g2}	temperature of ground at 2 m depth ..... °C
$T_{wa,out}$	outlet average water-antifreeze solution temperature of HGHE ..... °C
$T_{wa,in}$	inlet average water-antifreeze solution temperature of HGHE ..... °C
$T_{air,out}$	average air temperature leaving condenser unit °C
$T_{air,in}$	average air temperature entering condenser unit ..... °C
y	calculated neural network output
w	total uncertainty in the measurement of the mass flow rate ..... %
$\dot{W}_c$	power input to compressor ..... kW
$\dot{W}_p$	total power input to water-antifreeze solution circulating pump ..... kW
$\dot{W}_{cf}$	power input to condenser fan ..... kW
$\dot{V}_{air}$	volumetric flow rate of air ..... m^3/s
ρ_{air}	density of air ..... kg/m^3

Superscripts

mea	measured
pre	predicted
1	for HGHE1
2	for HGHE2

will be highly important and essential. Numerous prediction techniques, which mainly include multiple linear regression (MLR), autoregressive integrated moving average (ARIMA), grey model (GM) and artificial neural network (ANN), have been formerly studied in the heat pump performance forecasting. ANN is widely accepted as a technology offering an alternative way to tackle complex problems in actual situations. The advantage of ANN with respect to other models is their ability of modelling a multivariable problem given by the complex relationships between the variables and can extract the implicit non-linear relationships among these variables by means of 'learning' with training data.

ANN modelling of energy systems has been recently studied by numerous investigators, as summarized by Kalogirou [3]. Bechtler et al. [4] presented an ANN model for predicting the steady-state performance of a vapour compression heat pump. Swider [5] compared ANNs and empirically based steady-state models for vapour compression liquid chillers. Arcaklioglu et al. [6] determined the performance of a vapour compression heat pump using ANNs. Ertunc and Hosoz [7] used the ANN approach to predict various performance parameters of an R134a refrigeration system employing an evaporative condenser.

This paper describes the applicability of SWP-ANN to predict performance of a horizontal GCHP with R-22 as the refrigerant for a heating mode. For this aim, an experimental GCHP system (two different GHE) was set up and tested in winter conditions. Then, utilizing some of experimental data for training, a SWP-ANN model for the system based on the back propagation algorithm was developed. We compare ANNs results with the SWP-ANN results. The simulation results show that the SWP based networks can be used an alternative way in these systems.

2. System description

The schematic of the horizontal GCHP system constructed for space heating is illustrated in Fig. 1. Table 1 summarizes the main components specification and characteristics of the GCHP system. The experimental set-up consists of three main components:

- Horizontal ground heat exchanger (HGHE),
- heat pump unit equipment,
- auxiliary equipment.

There have been two GHEs installed at the University of Firat. Each consists of a high density polyethylene tube, 0.016 m diameter. The HGHE1 and HGHE2 are made as a single pass straight tube, buried at the depth of 1 and 2 m. The heat exchangers were been buried in the native ground. To allow for measurement of the circulating water-antifreeze solution and ground temperature a number of T-type thermocouples were installed. The pipe–ground interface temperature is measured in a similar fashion to the water-antifreeze solution-temperature measurement; except that thermal insulation is not used here since the thermocouple should have good contact with both the pipe and the ground.

The heat transfer from Earth to the heat pump or from the heat pump to Earth is maintained with the fluid or water-antifreeze solution circulated through the HGHEs. The fluid transfers its heat to refrigerant fluid in the evaporator (the water-antifreeze solution to refrigerant heat exchanger). The refrigerant, which flows through other closed loop in the heat pump, evaporates by absorbing heat from the water-antifreeze solution circulated through the evaporator and then enters the hermetic compressor. The refrigerant is compressed by the compressor and then enters the condenser, where it condenses. After the

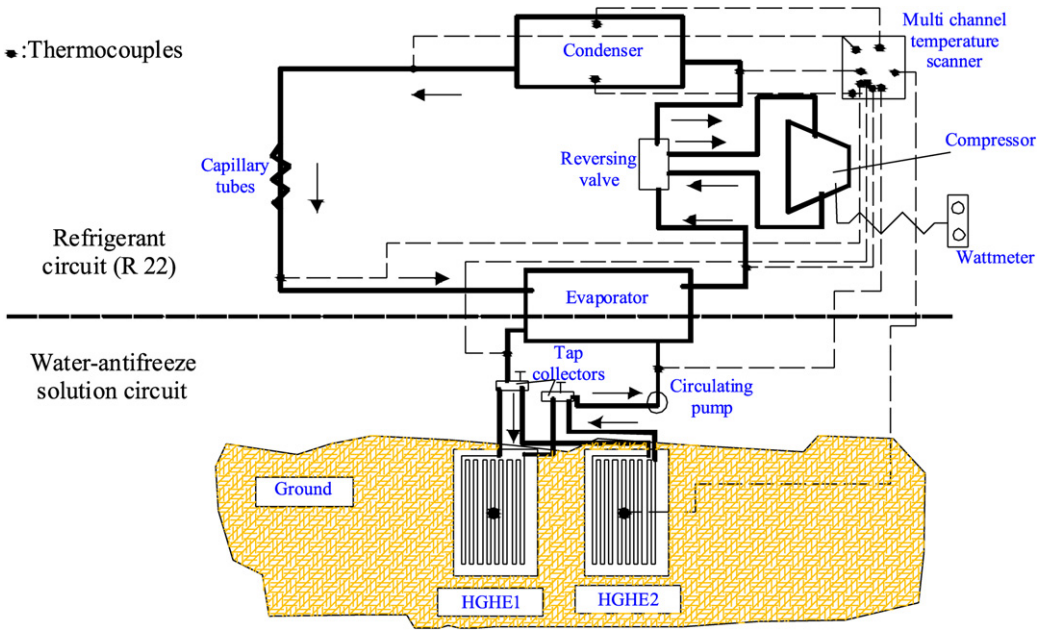

Fig. 1. Schematic diagram of the experimental apparatus.

Table 1
Technical features of the experimental set-up

Location: Elazığ, Turkey (lat. 38.41 °N; long. 39.14 °E)	
Room information:	
Window area	2.24 m^2
Wall area	34.63 m^2
Floor area	16.24 m^2
Ceiling area	16.24 m^2
Comfort temperature	293 K
Dimensions of the building	55.21 m^3
Heat pump information:	
Capacity	4.279 kW
Compressor type	Hermetic
Evaporator type	TT3; copper and inner cooling aluminium
Condenser type	HS 10; friterm
Compressor power input	2 HP; 1.4 kW
Compressor volumetric flow rate	7.6 m^3/h
Compressor rotation speed	2900 tr/mn
Condenser fan	2350 m^3/h, 145 W
Evaporating temperature	0 °C
Condensing temperature	54.5 °C
Refrigerant type	R-22
Ground heat exchanger information:	
Configuration type	Horizontal
Pipe material	Polyethylene, PX-b Cross Link
Length of pipe	50 m × 2
Pipe diameter	0.016 m
Piping depth	1 and 2 m
Pipe distance	0.3 m
Circulating pump information:	
Type	Alarko, NPVO-26-P
Powers	40, 62, 83 W

refrigerant leaves the condenser, the capillary tube provides almost 10 °C superheat that essentially gives a safety margin to reduce the risk of liquid droplets entering the compressor. A fan blows across the condenser to move the warmed air of the room. A non-toxic propylene glycol solution, 25% by weight, was circulated through the HGHE. In the heating season, the heat exchange fluid (water-antifreeze solution) in the HGHE loop collects heat from the earth and transfers that heat to the room. After the heat exchange fluid absorbs heat from the ground, the closed loop GHEs circulates the heat exchange fluid through pipes (see Fig. 1).

As can be seen in Fig. 1, the collector valve allows for varying the circulating water-antifreeze solution flow rate. The flow rate of the circulated water-antifreeze solution through the closed loop GHE was measured by using a rotameter and controlled by a hand-controlled tap mounted on the collector. Anemometer has been used to measure the circulating air flow velocity. The electric power consumed by the system (compressor, water-antifreeze circulating pump and fan) was measured by means of wattmeter. The inlet and outlet temperatures of the R-22 in the condenser, compressor and evaporator were measured with T-type (copper-constantan) thermocouples. In addition, temperatures of the circulated water-antifreeze solution at inlet and outlet of the HGHEs and evaporator (Fig. 1) were measured. The ambient and indoor air temperatures were measured with thermometers. The inlet and outlet pressures of the compressor and evaporator were measured by using Bourdon tube type manometers.

The heating and cooling loads of the test room were 2.5 and 3.1 kW at design conditions, respectively. The compressor and other part of the experimental system were selected the according to the heating and cooling load of test room from the manufacturer's catalog data. The COP of the GCHP system is calculated as Refs. [1,2].

3. Experimental analysis and uncertainty

Experimental performances were performed to verify the results from the ANN approach. The experimental temperature results are given in Figs. 2 and 3. Fig. 2 shows the daily variation of ($T_{air1,out}$), ($T_{air1,in}$), ($T_{wa1,out}$), ($T_{wa1,in}$), (T_{g1}), (T_a) and (T_i) in the case of using HGHE1. The room temperature is set to a range of 21–24 °C by using a digital thermostat. The compressor and circulating pump work in this temperature range. When the room temperature exceeds 24 °C, only condenser fan works, and therefore the room temperature decreases again. When the room temperature decreases below 21 °C, the compressor and circulating pump restart up. As the compressor and circulating pump run, the outlet and inlet water-antifreeze solution temperature drastically drop.

However, the mentioned solution temperatures increase when they do not work. Fig. 3 indicates the daily variation of ($T_{air2,out}$), ($T_{air2,in}$), ($T_{wa2,out}$), ($T_{wa2,in}$), (T_{g2}), (T_a) and (T_i) in

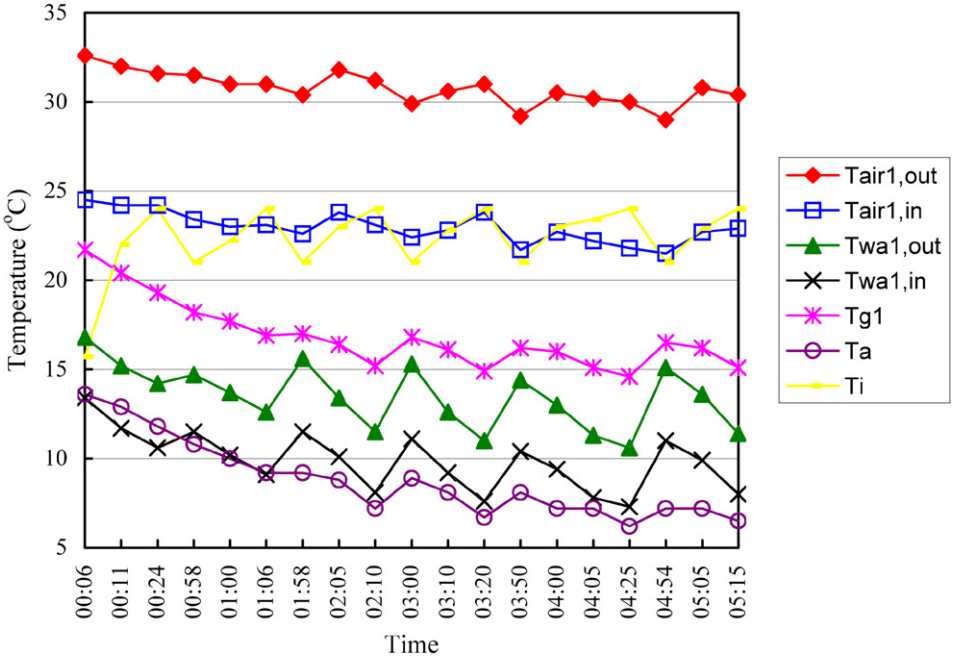

Fig. 2. The daily variation of various temperatures for the HGHE1.

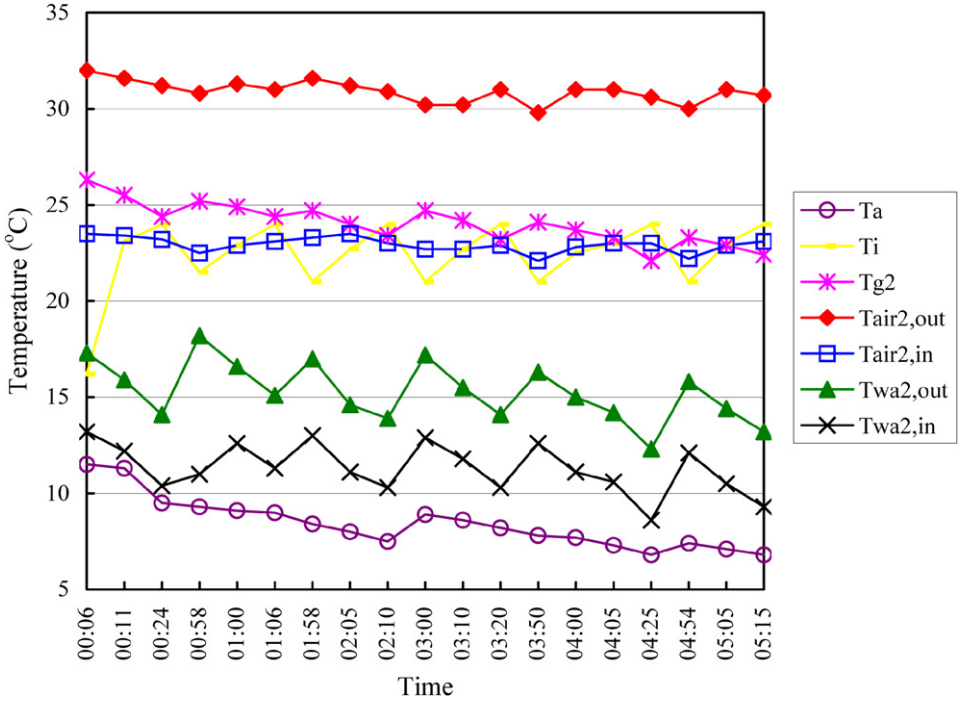

Fig. 3. The daily variation of various temperatures for the HGHE2.

the case of using HGHE2. It can be seen from Fig. 3 that the trends in ($T_{\text{air2,out}}$), ($T_{\text{air2,in}}$), ($T_{\text{wa2,out}}$), ($T_{\text{wa2,in}}$), (T_{g2}), (T_{a}) and (T_{i}) are similar to those given in Fig. 2.

The COP of the GCHP system was calculated by Refs. [1,2]. The COP increases with increasing the buried depth of HGHE. Thus, the much more proper HGHEs design gives higher enhancement rates for COP.

An important issue is the accuracy of the measured data as well as the results obtained by experimental studies. Uncertainty is a measure of the "goodness" of a result. Without such a measure, it is impossible to judge the fitness of the value as a basis for making decisions relating to health, safety, commerce or scientific excellence.

The result R is a given function in terms of the independent variables. Let w_R be the uncertainty in the result and $w_1, w_2, \ldots, w_n$ be the uncertainties in the independent variables. The result R is a given function of the independent variables $x_1, x_2, x_3, \ldots, x_n$. If the uncertainties in the independent variables are all given with same odds, then uncertainty in the result having these odds is calculated by [8]

$$w_R = \left[\left(\frac{\partial R}{\partial x_1} w_1\right)^2 + \left(\frac{\partial R}{\partial x_2} w_2\right)^2 + \cdots + \left(\frac{\partial R}{\partial x_n} w_n\right)^2\right]^{1/2} \quad (1)$$

It is important that all uncertainties used in Eq. (1) can be evaluated at the same confidence level. The uncertainty estimates in the COP can be calculated from Eq. (1) as

$$\begin{aligned} w_{\text{COP}} = \Bigg[&\left(\frac{\partial \text{COP}}{\partial \rho_{\text{air}}} w_{\rho_{\text{air}}}\right)^2 + \left(\frac{\partial \text{COP}}{\partial \dot{V}_{\text{air}}} w_{\dot{V}_{\text{air}}}\right)^2 \\ &+ \left(\frac{\partial \text{COP}}{\partial C_{\text{p,air}}} w_{c_{\text{p,air}}}\right)^2 + \left(\frac{\partial \text{COP}}{\partial T_{\text{air,out}}} w_{T_{\text{air,out}}}\right)^2 \\ &+ \left(\frac{\partial \text{COP}}{\partial T_{\text{air,in}}} w_{T_{\text{air,in}}}\right)^2 + \left(\frac{\partial \text{COP}}{\partial \dot{W}_{\text{c}}} w_{\dot{W}_{\text{C}}}\right)^2 \\ &+ \left(\frac{\partial \text{COP}}{\partial \dot{W}_{\text{p}}} w_{\dot{W}_{\text{p}}}\right)^2 + \left(\frac{\partial \text{COP}}{\partial \dot{W}_{\text{cf}}} w_{\dot{W}_{\text{cf}}}\right)^2\Bigg]^{1/2} \end{aligned} \quad (2)$$

The total uncertainties of the measurements are estimated to be ±2.89% for the water-antifreeze temperatures and refrigerant temperatures, ±2.75% for pressures, ±4.35% for power inputs to the compressor, condenser fan and circulating pump, and ±3.00% for electric currents. Uncertainty in reading values of the table is assumed to be ±0.20%. The overall uncertainty for COP calculations was found to be 3.94 % for the R-22 test. The uncertainty of COP is small enough.

4. Artificial neural networks (ANNs)

An ANN is an information processing idea that is inspired by the way biological nervous systems, such as the brain, process information. The key element of this idea is the novel structure of the information processing system. It is composed of a large number of highly interconnected processing elements (neurones) working in unison to solve specific problems. A schematic diagram for an artificial neuron model is shown in Fig. 4.

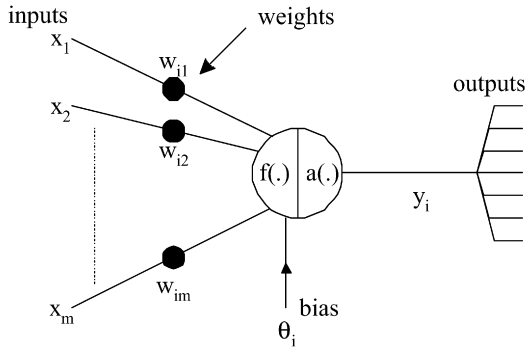

Fig. 4. Artificial neuron model.

These neurons are connected with connection link. Each link has a weight that multiplied with transmitted signal in network. Each neuron has an activation function to determine the output. There are many kind of activation function. Usually nonlinear activation functions such as sigmoid, step are used. Neural Network's are trained by experience, when applied an unknown input to the network it can generalize from past experiences and product a new result [9,10]. The output of the neuron *net* is given by Eq. (3).

$$y(t+1) = a\left(\sum_{j=1}^{m} w_{ij} x_j(t) - \theta_i\right) \quad \text{and}$$

$$f_i \underline{\underline{\Delta}} net_i = \sum_{j=1}^{m} w_{ij} x_j - \theta_i \quad (3)$$

where, $X = (X_1, X_2, \ldots, X_m)$ represent the m input applied to the neuron, W_i represent the weights for input X_i, θ_i is a bias value, $a(.)$ is activation function.

There are numerous algorithms available for training neural network models; most of them can be viewed as a straightforward application of optimization theory and statistical estimation. Most of the algorithms used in training artificial neural networks are employing some form of gradient descent. This is done by simply taking the derivative of the cost function with respect to the network parameters and then changing those parameters in a gradient-related direction. The most popular of them is the back propagation algorithm, which has different variants. Standard back propagation is a gradient descent algorithm. It is very difficult to know which training algorithm will be the fastest for a given problem, and the best one is usually chosen by trial and error. An ANN with a back propagation algorithm learns by changing the connection weights, and these changes are stored as knowledge.

5. Statistical data weighting pre-processing (SWP) and modeling of the system

The proposed method involves a two-stage system in which an ANN modeling system and SWP are hybridized. In the first stage, normalization of the input data set is conducted and normalized data are weighted in the interval [0, 1] using statistical weighting pre-processing. After this pre-processing step, the

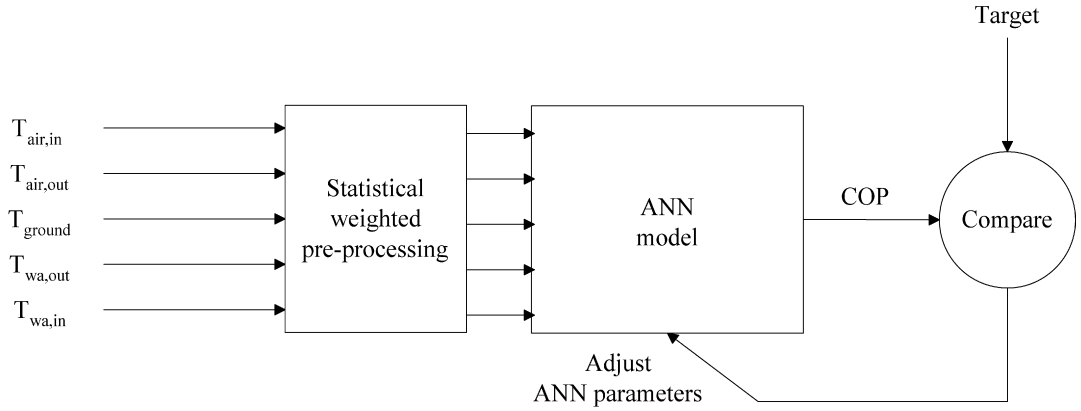

Fig. 5. Proposed model block diagram.

weighted data set was presented to the main modeling unit. The second stage uses ANN to model weighted data.

The procedure of the proposed statistical weighed pre-processing stage is defined as follows;

Assume that the data set which is going to be used for modeling the GCHP system is composed of $L \times N$ matrix. Where L indicates the number of input variables and N indicates the number of samples per variable. The algorithm of the proposed statistical weighting pre-processing system is given as following:

(1) Determine the number of the input variables (L)
(2) For each input variable ($i = 1, 2, 3, \ldots, L$), do:
  (2.1) Calculate the standard deviation of the input variable i:

$$std(X_i) = \sqrt{\frac{1}{N}\sum_{k=1}^{N}\left(X_{k,i} - \mu(X_i)\right)^2} \tag{4}$$

  where $\mu(X_i)$ is the mean value of the ith input variable for N samples and can be calculated as following:

$$\mu(X_i) = \frac{1}{N}\sum_{k=1}^{N} x_k \tag{5}$$

  (2.2) Calculate the weight for ith input variable as given:

$$w_i = \frac{\mu(X_i)}{std(X_i)} \tag{6}$$

(3) Update the input variables with the calculated w_i weights.

$$new(X_i) = w_i * old(X_i) \tag{7}$$

In the statistical weighting pre-processing, the training samples are used for determining the effect of each input variable to the system modeling procedure. The variable which has more influence on the system modeling will get the more weights than the other input variables. Thus, each variable takes new values according to its old values. Moreover, it is assumed that the input variable which has less deviation for N samples is the best for modeling the examined system. But, if a variable changes abruptly, that variable is assumed to be less important in using the modeling procedure.

There are many types of ANN architectures in the literature; however, multi-layer feed-forward neural network is the most widely used for prediction. A multi-layer feed-forward neural network typically has an input layer, an output layer, and one or more hidden layers [3]. In multi-layer feed-forward networks, neurons are arranged in layers and there is a connection among the neurons of other layers. The input signals are applied to the input layer, the output layer contributes to the output signal directly. Other layers between input and output layers are called hidden layers. Input signals are propagated in gradually modified form in the forward direction, finally reaching the output layer [11].

In this study, the model has five input variables and one output variable. Air temperature entering the condenser unit ($T_{\mathrm{air,in}}$), air temperature leaving the condenser unit ($T_{\mathrm{air,out}}$), water-antifreeze solution entering the HGHEs ($T_{\mathrm{wa,in}}$), water-antifreeze solution leaving the HGHEs ($T_{\mathrm{wa,out}}$) and ground temperatures at 1 and 2 meters (T_{g1} and T_{g2}) constitutes the input variables of the model. The COP of the system is the output variable of the ANN model. The inputs of the model are normalized in the (0, 1) range with the SWP. The output values are not normalized.

The block diagram of the proposed model is given in Fig. 5. As can be seen from the block diagram; ANN model is adjusted, or trained, so that a particular input leads to a specific target output. Here, the ANN model is adjusted, based on a comparison of the output and the target, until the model output matches the target. Typically, many such input/target output pairs are used to train a model.

The training parameters and the structure of the ANN used in this study are as shown in Table 2. These were selected for the best performance, after several different experiments, such as the number of hidden layers, the size of the hidden layers, value of learning rate, and type of the activation functions.

6. Results and discussion

In order to indicate the efficiency of the proposed SWP and ANN structure for modeling purposes, a computer program was

Table 2
ANN architecture and training parameters

Architecture	
The number of layers	3
The number of neuron on the layers	Input: 5 Hidden: 5, 6, 7, 8, 9, 10, 11, 12, 13, 14 and 15 Output: 1
The initial weights and biases	Random
Activation functions	Tangent Sigmoid
Training parameters	
Learning rule	Scaled Conjugate Gradient (SCG)
Learning rate	0.8
Mean-squared error	1e−07

performed under MATLAB (version 5.3. The MathWorks Inc., USA) environment using the neural network toolbox.

The optimal model parameters such as different training algorithms, initial weights and activation function of the ANN were investigated elsewhere [6,10] and out of scope of this paper. Here, we only investigated the effect of the SWP of the input data set on performance when modeling with ANN. Moreover, a variable number of neurons (from 5 to 15) were used in the hidden layer to observe as any performance improvement can be obtained with the proposed modeling system. Thus, we constructed the ANN model with the parameters which are given in Table 2. The data set was divided into two separate data sets randomly—the training data set and the testing data set. The training data set was used to train the ANN model, whereas the testing data set was used to verify the accuracy and the effectiveness of the trained ANN model for GCHP system (for HGHE1 and HGHE2). The adequate functioning of the ANN depends on the sizes of the training set and test set. The data set for the COP of GCHP system (for HGHE1 and HGHE2) available included 38 data patterns. From these, 25 data patterns were used for training the ANN, and the remaining 13 patterns were used as the test data set for trained ANN model.

Model validation is the process by which the input vectors from input/output data sets on which the ANN was not trained, are presented to the trained model, to see how well the trained model predicts the corresponding data set output values. Some statistical methods, such as the root-mean squared (RMS), the coefficient of multiple determinations (R^2) and the coefficient of variation (cov) may be used to compare predicted and actual values for model validation.

The error can be estimated by the RMS, defined as [10,12]:

$$\mathrm{RMS} = \sqrt{\frac{\sum_{m=1}^{n}(y_{\mathrm{pre},m} - t_{\mathrm{mea},m})^2}{n}} \tag{8}$$

In addition, the coefficient of multiple determinations (R^2) and the coefficient of variation (cov) in percent are defined as follows:

$$R^2 = 1 - \frac{\sum_{m=1}^{n}(y_{\mathrm{pre},m} - t_{\mathrm{mea},m})^2}{\sum_{m=1}^{n}(t_{\mathrm{mea},m})^2} \tag{9}$$

Table 3
Statistical values of COP for ANN

Algorithm-neurons	RMS	cov	R^2
SCG5	0.472323	14.521747	0.979375
SCG6	0.074953	2.220088	0.999871
SCG7	0.217507	6.327536	0.996017
SCG8	0.452977	11.827146	0.986067
SCG9	0.111438	3.170915	0.998996
SCG10	0.366284	10.730821	0.988589
SCG11	0.171011	4.747563	0.997748
SCG12	0.255057	7.544056	0.994344
SCG13	0.163817	4.681177	0.997812
SCG14	0.148872	4.208714	0.998229
SCG15	0.123272	3.495283	0.998779

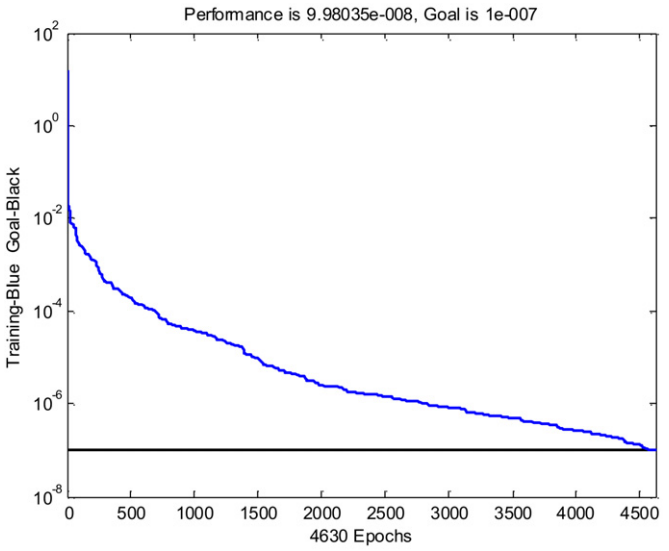

Fig. 6. Variation of mean-square error with training epochs for SCG6 topology. (For interpretation of the references to color in this figure, the reader is referred to the web version of this article.)

$$\mathrm{cov} = \frac{\mathrm{RMS}}{|\bar{t}_{\mathrm{mea},m}|}100 \tag{10}$$

where n is the number of data patterns in the independent data set, $y_{\mathrm{pre},m}$ indicates the predicted, $t_{\mathrm{mea},m}$ is the measured value of one data point m, and $\bar{t}_{\mathrm{mea},m}$ is the mean value of all measured data points.

The computer simulations are carried out as the following manner; first; ANN topologies with various number of hidden layer neurons are trained without SWP normalized inputs. But for the sake of justice, we have normalized the ANN inputs by dividing the each sample with a constant value. Therefore, the input vector of the ANN was normalized to (0, 1) range. The prediction results of the ANN models are given in Table 3. The training performance of the ANN (SCG6 topology) is given in Fig. 6 where the variation of mean-square error with training epochs is illustrated. Fig. 7 also shows the comparison of calculated and ANN predicted COP values of GCHP system for SCG6 and the model error for each test sample is shown in Fig. 8. Second, the ANN topologies with various number of hidden layer neurons are trained with the statistical weighting pre-processed inputs. The related test results (RMS,

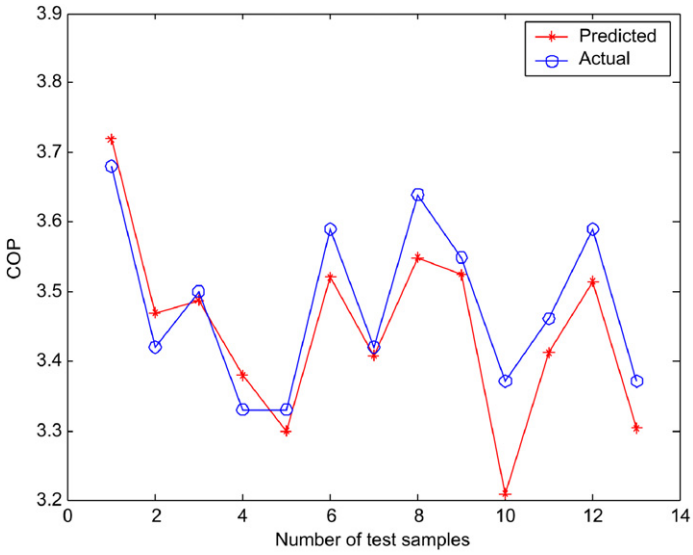

Fig. 7. Comparison of calculated and ANN predicted values of GCHP system COP for SCG6.

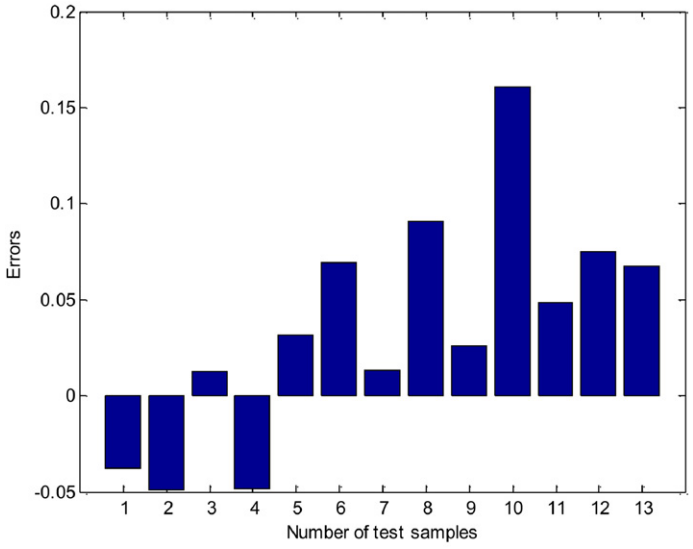

Fig. 8. Error for each sample for SCG6.

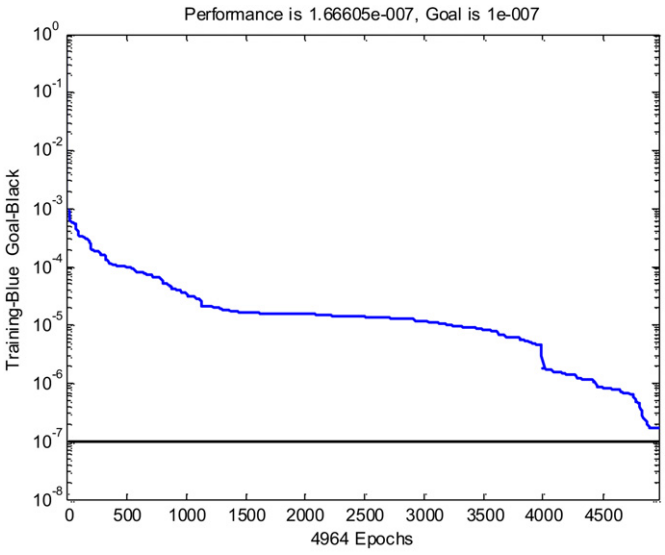

Fig. 9. Variation of mean-square error with training epochs for SWP-SCG6 topology. (For interpretation of the references to color in this figure, the reader is referred to the web version of this article.)

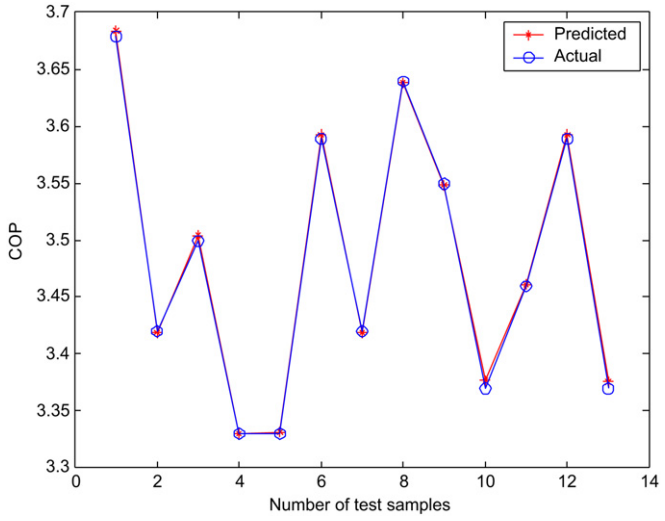

Fig. 10. Comparison of calculated and predicted COP values for SWP-SCG6.

cov and R^2) are represented in Table 4. The decrease of the training performance during the training process of SWP-SCG6 topology is shown in Fig. 9. In this figure the variation of mean-square error with training epochs is given. The input variables against to the output variables of SWP-SCG6 topology for the test data set are also shown in Fig. 10. The errors of the SWP-SCG6 model predictions for each test sample are also given in Fig. 11.

One observes from both cases (ANN with SWP and only ANN) by decreasing the number of hidden neurons the training accuracy improves, as indicated by the smaller RMS and cov values and R^2-values approaching 1 (Tables 3 and 4). On the other hand, beyond a certain point the errors obtained begin to increase together with the complexity of the ANN as the larger the number of hidden neurons the more complex the network is. So, the convergence to the target error rate (1e−007) takes more iteration. This situation is very time consuming. From the statistical data presented in Tables 3 and 4, for COP values SWP-SCG6 algorithm with six neurons in the hidden layer appeared to be most optimal topology. This topology gained 0.002665 RMS value, 0.076557 cov value and, 0.999999 R^2 value, respectively. These values are really promising. The rest of the SWP based ANN modeling results are also promising. The R^2 value of each topology is 0.9999 and RMS and cov values are considerably small. It is observed during the several runs of the computer simulation that the convergence of the SWP-ANN takes more iteration. But the average prediction error is quite small. This situation can be seen in Fig. 11.

The statistical results of the first stage of the computer simulation are given in Table 4. As it is aforementioned, this stage involves the usage of only ANN structure for modeling purposes. The related prediction results and structural information

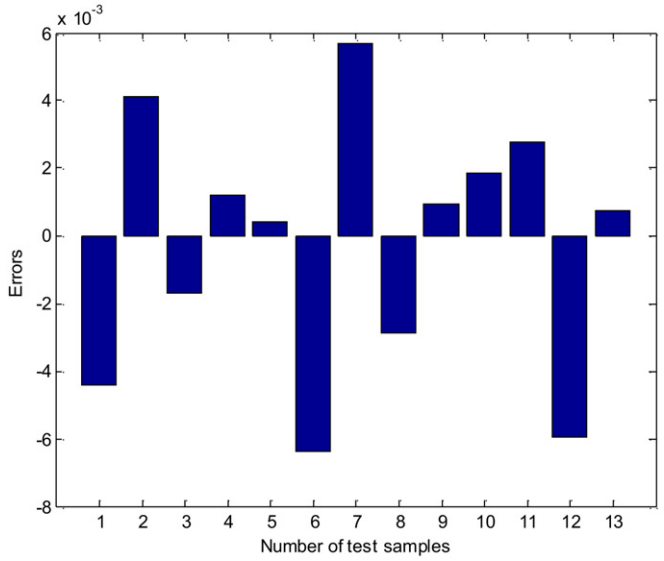

Fig. 11. Error for each sample for SWP-SCG6.

Table 4
Statistical values of COP for ANN with SWP normalization

Algorithm-neurons	RMS	cov	R^2
SWP-SCG5	0.004989	0.143290	0.999997
SWP-SCG6	0.002665	0.076557	0.999999
SWP-SCG7	0.004903	0.140958	0.999998
SWP-SCG8	0.006267	0.179854	0.999996
SWP-SCG9	0.002734	0.078810	0.999999
SWP-SCG10	0.002835	0.081417	0.999999
SWP-SCG11	0.003513	0.100882	0.999998
SWP-SCG12	0.005919	0.169903	0.999997
SWP-SCG13	0.007908	0.227402	0.999994
SWP-SCG14	0.013958	0.175948	0.999927
SWP-SCG15	0.013665	0.391664	0.999984

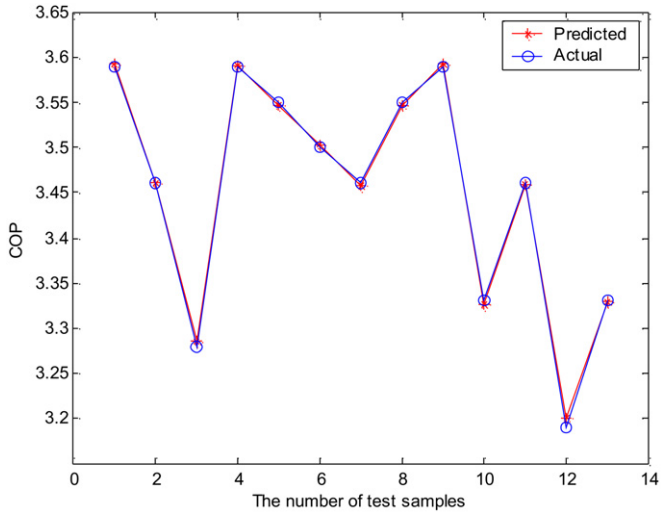

Fig. 12. Comparison of calculated and predicted COP values for SWP-SCG6 (the first part of the data set).

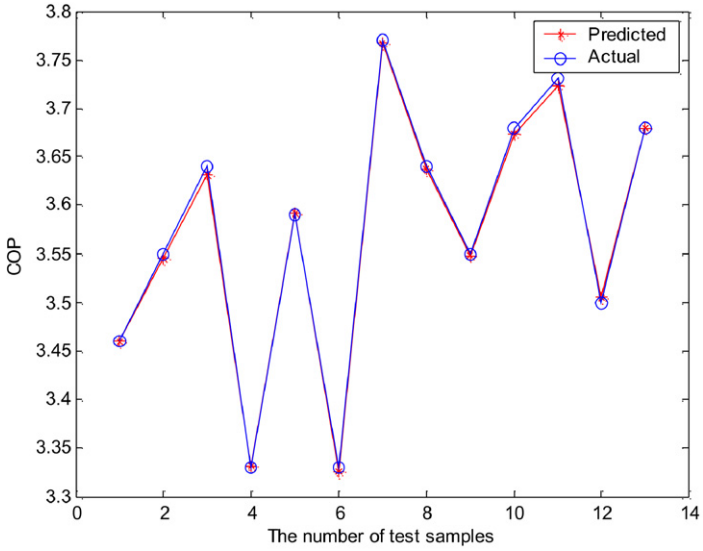

Fig. 13. Comparison of calculated and predicted COP values for SWP-SCG6 (the second part of the data set).

of the ANN are given in subsequent graphics. One observes from Table 3, where this table gave us the statistical validation of the proposed modeling, the most appropriate ANN topology is SCG6. 0.074953 RMS value, 2.220088 cov value and 0.999871 R^2 value is obtained for test patterns. The rest of the results are obtained for the related ANN structures. These results are not promising when compared with the results which were obtained with SWP-ANN structure. The convergence of these structures is not taken more iteration. The running time of the computer simulation of these structures is less than SWP-ANN structure.

Moreover, the efficiency of the proposed method was demonstrated by using the 3-fold cross validation test. In 3-fold cross validation dataset is randomly split into three exclusive subsets $(X_1, \ldots, X_3)$ of approximately equal size and the holdout method is repeated 3 times. These subsets contain 13, 13 and 12 samples $(13 + 13 + 12 = 38)$ respectively. At each time, one of the three subsets is used as the test set and the other two subsets are put together to form a training set. The advantage of this method is that it is not important how the data is divided. Every data point appears in a test set only once, and appears in a training set 2 times. Therefore, the verification of the efficiency of the proposed method against to the over-learning problem should be demonstrated. The 3-fold cross validation test results were shown in Figs. 12, 13 and 14, respectively. The first subset of the cross validation test was shown in Fig. 12 and the second part of the data set and the predicted COP values were given in Fig. 13 and finally the last part of the data set was already given in Fig. 14.

7. Conclusions

The objective of this work is to improve the performance of an ANN with a SWP method to learn to predict GCHP systems with the minimum data set. To evaluate the effectiveness of our proposal (SWP-ANN), a computer simulation is devel-

Table 5
Experimental data's at HGHE1 situation

HGHE1		Time (h)	Input variables						Output variable
			$T_{wa1,in}$ (°C)	$T_{wa1,out}$ (°C)	T_{g1} (°C)	T_{g2} (°C)	$T_{air1,out}$ (°C)	$T_{air1,in}$ (°C)	COP
Training samples	1	00:06	13.4	16.8	21.7	28.2	32.6	24.5	3.59
	2	00:11	11.7	15.4	20.4	26.8	32	24.2	3.46
	3	00:24	10.6	14.2	19.3	25.6	31.6	24.2	3.28
	4	00:58	11.5	14.7	18.2	24.8	31.5	23.4	3.59
	5	01:10	10.2	13.7	17.7	24.2	31	23	3.55
	6	01:20	9.1	12.6	16.9	23.4	31	23.1	3.5
	7	01:58	11.5	15.6	17	23.9	30.4	22.6	3.46
	8	02:07	10.1	13.4	16.4	23.3	31.8	23.8	3.55
	9	02:15	8.1	11.5	15.2	21.9	31.2	23.1	3.59
	10	03:00	11.1	15.3	16.8	23.9	29.9	22.4	3.33
	11	03:10	9.2	12.6	16.1	23	30.8	22.8	3.46
	12	03:20	7.6	11	14.9	21.7	31	23.8	3.19
	13	03:50	10.4	14.4	16.2	23.4	29.2	21.7	3.33
	14	04:00	9.4	13	16	23.1	30.5	22.7	3.46
	15	04:07	7.8	11.3	15.1	22.1	30.2	22.2	3.55
	16	04:25	7.3	10.6	14.6	21.6	30	21.8	3.64
	17	04:54	11	15.1	16.5	23.8	29	21.5	3.33
	18	05:05	9.9	13.6	16.2	23.5	30.8	22.7	3.59
	19	05:15	8	11.4	15.1	22.3	30.4	22.9	3.33

Table 6
Experimental data's at HGHE2 situation

HGHE2		Time (h)	Input variables						Output variable
			$T_{wa2,in}$ (°C)	$T_{wa2,out}$ (°C)	T_{g1} (°C)	T_{g2} (°C)	$T_{air2,out}$ (°C)	$T_{air2,in}$ (°C)	COP
Training samples	20	00:06	13.2	17.3	19.7	26.3	32	23.5	3.77
	21	00:11	12.2	15.9	19.1	25.5	31.6	23.4	3.64
	22	00:24	10.4	14.1	18	24.4	31.2	23.2	3.55
	23	00:58	11	18.2	18.5	25.2	30.8	22.5	3.68
	24	01:10	12.6	16.6	18.3	24.9	31.3	22.9	3.73
	25	01:20	11.3	15.1	17.8	24.4	31	23.1	3.5
Testing samples	26	01:58	13	17	18.1	24.7	31.6	23.3	3.68
	27	02:07	11.1	14.6	17.4	24	31.2	23.5	3.42
	28	02:15	10.3	13.9	16.9	23.4	30.9	23	3.5
	29	03:00	12.9	17.2	18.1	24.7	30.2	22.7	3.33
	30	03:10	11.8	15.5	17.7	24.2	30.2	22.7	3.33
	31	03:20	10.3	14.1	16.9	23.2	31	22.9	3.59
	32	03:50	12.6	16.3	17.5	24.1	29.8	22.1	3.42
	33	04:00	11.1	15	17.2	23.7	31	22.8	3.64
	34	04:07	10.6	14.2	16.9	23.3	31	23	3.55
	35	04:25	8.6	12.3	15.8	22.1	30.6	23	3.37
	36	04:54	12.1	15.8	17	23.3	30	22.2	3.46
	37	05:05	10.5	14.4	16.6	22.9	31	22.9	3.59
	38	05:15	9.3	13.2	16.1	22.4	30.7	23.1	3.37

oped on MATLAB environment. We compare our results with the ANN results. In related tables, these comparisons can be seen. Some statistical methods, such as the root-mean squared (RMS); the coefficient of multiple determinations (R^2) and the coefficient of variation (cov) are used to compare predicted and actual values for model validation. The R^2-values are about 0.9999, which can be considered as very promising. The simulation results show that the SWP based networks can be used an alternative way in these systems.

This paper shows that the values predicted with the SWP-ANN, especially with the back propagation learning algorithm along with feed forward, can be used to predict the performance of the GCHP system quite accurately. Therefore, instead of limited experimental data found in literature, faster and simpler solutions are obtained using hybridized structures such as SWP-ANN.

It can therefore be concluded that it is possible to train a suitable neural network to model a GCHP system, which can

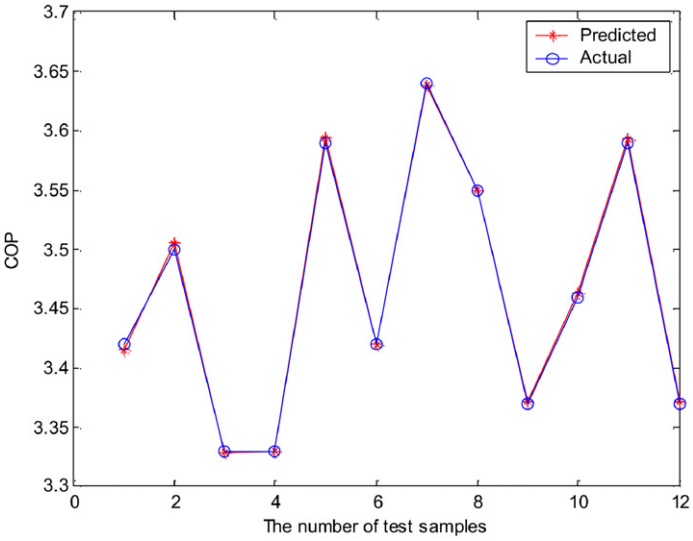

Fig. 14. Comparison of calculated and predicted COP values for SWP-SCG6 (the third part of the data set).

be used to predict the performance of the system under any ambient and soil conditions. Future studies will concentrate on applications in predicting the fault diagnosis of GCHP systems.

Appendix

The training and testing samples (data) are given in Tables 5 and 6, respectively.

References

[1] M. Inalli, H. Esen, Experimental thermal performance evaluation of a horizontal ground-source heat pump system, Appl. Thermal Engrg. 24 (14–15) (2004) 2219–2232.
[2] H. Esen, M. Inalli, M. Esen, Technoeconomic appraisal of a ground source heat pump system for a heating season in eastern Turkey, Energy Convers. Management 47 (9–10) (2006) 1281–1297.
[3] S.A. Kalogirou, Application of artificial neural-networks for energy systems, Appl. Energy 67 (1–2) (2000) 17–35.
[4] H. Becthler, M.W. Browne, P.K. Bansal, V. Kecman, Neural networks—a new approach to model vapour-compression heat pumps, Int. J. Energy Res. 25 (7) (2001) 591–599.
[5] D.J. Swider, A comparison of empirically based steady-state models for vapour-compression liquid chillers, Appl. Thermal Engrg. 23 (5) (2003) 539–556.
[6] E. Arcaklioglu, A. Erisen, R. Yilmaz, Artificial neural network analysis of heat pumps using refrigerant mixtures, Energy Convers. Management 45 (11–12) (2004) 1917–1929.
[7] H.M. Ertunc, M. Hosoz, Artificial neural network analysis of a refrigeration system with an evaporative condenser, Appl. Thermal Engrg. 26 (5–6) (2006) 627–635.
[8] J.P. Holman, Experimental Methods for Engineers, sixth ed., McGraw–Hill Book Co, Singapore, 1994.
[9] C.L. Zhang, Generalized correlation of refrigerant mass flow rate through adiabatic capillary tubes using artificial neural network, Int. J. Refrigeration 28 (4) (2005) 506–514.
[10] A. Sencan, S.A. Kalogirou, A new approach using artificial neural networks for determination of the thermodynamic properties of fluid couples, Energy Convers. Management 46 (15–16) (2005) 2405–2418.
[11] M.A. Akcayol, C. Cinar, Artificial neural network based modeling of heated catalytic converter performance, Appl. Thermal Engrg. 25 (14–15) (2005) 2341–2350.
[12] H. Becthler, M.W. Browne, P.K. Bansal, V. Kecman, New approach to dynamic modelling of vapour-compression liquid chillers: artificial neural networks, Appl. Thermal Engrg. 21 (9) (2001) 941–953.